Momentum dependence of generalised oscillator strengths of atomic K shells using the local plasma approximation

1990 J. Phys. B: At. Mol. Opt. Phys. 23 2543

(http://iopscience.iop.org/0953-4075/23/15/021)

J. Phys. B: At. Mol. Opt. Phys. **23** (1990) 2543-2551. Printed in the UK

Momentum dependence of generalised oscillator strengths of atomic K shells using the local plasma approximation†

C M Kwei‡ and C J Tung§

‡ Department of Electronics Engineering, National Chiao Tung University, Hsinchu, Taiwan

§ Institute of Nuclear Science, National Tsing Hua University, Hsinchu, Taiwan

Received 5 December 1989, in final form 13 March 1990

Abstract. Previously, we have calculated atomic generalised oscillator strengths at zero momentum transfer using the local plasma approximation. In this work, we have extended our calculations to non-zero momentum transfer for the atomic K shell. Basically, we have adopted similar formulations to those developed previously, however, parameters here were allowed to be momentum dependent. A pseudo-electron density distribution derived from the exact generalised oscillator strength data at zero momentum transfer was employed in the present work. This has several advantages over the Hartree-Slater electron density distribution employed previously. Calculated results of the generalised oscillator strengths at any momentum transfer and energy transfer for atoms up to sodium have been compared with theoretical data of the matrix element method. Fairly reasonable agreement was found for all cases.

1. Introduction

Atomic generalised oscillator strength (GOS) has been defined by Bethe for the stopping power of charged particles (Bethe 1930, 1933). The GOS embodies the dynamic response properties of atoms in terms of atomic excitation and ionisation spectra. It is a function of momentum and energy transfers incurred in the inelastic interactions between charged particles and atoms. In the limit of zero momentum transfer, the GOS approaches the optical oscillator strength.

Theoretical prediction of GOS follows one of two different approaches. The first involves a full matrix element evaluation utilising atomic wavefunctions obtained from quantum mechanical methods such as the Hartree-Fock-Slater (HFS) (McGuire 1971, Dehmer *et al* 1975, Inokuti *et al* 1978) and the hydrogenic (Walske 1952, 1956) methods. The second employs models which are in general simpler but lead to less accurate results. Among these models, the binary collision model (Gryzinski 1965a, b, c, Tung 1980) and the local plasma approximation (LPA) (Johnson and Inokuti 1983, Tung and Kwei 1985) are the most frequently quoted.

Previously (Kwei *et al* 1988), we have calculated atomic ionisation GOS at zero momentum transfer using the LPA with the HFS electron density distribution (Herman and Skillman 1963). The LPA has been proven to be useful in the determination of shellwise ionisation GOS contributed by individual subshells of atoms. The approach of the LPA began with a Drude-type response function for electrons in a small volume

† Research sponsored by the National Science Council of the Republic of China.

0953-4075/90/152543+09$03.50

around the nucleus of an atom in a given subshell. The atomic GOS of that subshell was then obtained by averaging the above space-varying response function over the entire volume occupied by the atom according to the electron density distribution of that subshell. Quantum excitations of electrons and plasma oscillations of local electron densities have both been taken into consideration. Such an approach has also been adopted by Tung *et al* (1988) in the determination of atomic mean excitation energies.

Application of the LPA for atomic K-shell GOS at non-zero momentum transfers is the subject of this work. Previous derivation in the LPA formulations is generally valid. However, a few modifications need to be made before the application of these formulations. These include allowing the ionisation fraction, plasma damping coefficient and resonant energy to be momentum dependent. In addition, a pseudo-electron density distribution derived using the exact GOS data at zero momentum transfer may be utilised to develop GOS at non-zero momentum transfers.

2. Theory

The atomic GOS is a quantity which characterises the dynamic response of atoms on their interactions with charged particles. For interacting atomic systems such as solids and liquids, this response is usually expressed in terms of the dielectric function of the bulk material. In the case of weakly interacting systems such as dilute gases, the dielectric function is approximately related to the GOS by the relation (Powell 1985)

$$\frac{\partial f}{\partial \omega}(k, \omega) \simeq \frac{2\omega Z}{\pi \omega_p^2} \operatorname{Im}(-1/\varepsilon(k, \omega)) \tag{1}$$

where $\partial f/\partial \omega$ is the differential GOS with respect to the energy transfer ω, ε represents the dielectric function, $\operatorname{Im}(-1/\varepsilon)$ denotes the energy loss function, k is the momentum transfer, Z is the atomic number, $\omega_p = (4\pi n)^{1/2}$ is the free electron plasma energy, and n is the electron density. Note that atomic units are used throughout this paper unless otherwise specified.

For a system composed of atoms having several subshells with different binding energies, the dielectric function is given by (Ritchie and Howie 1977, Raether 1980)

$$\varepsilon(k, \omega) = 1 + \sum_i \frac{\omega_{pi}^2}{\omega_{ki}^2 - \omega_{pi}^2 - \omega(\omega + i\gamma_{ki})} \tag{2}$$

where ω_{ki} represents the energy-momentum dispersive relation, $\omega_{pi} = (4\pi n_i)^{1/2}$ is the plasma energy and γ_{ki} is the momentum-dependent plasma damping coefficient, all associated with the ith subshell. The exact form of the dispersive relation is guided by its behaviour at two extremes. At the optical end, i.e. $k \to 0$, ω_{ki} approaches the effective plasma energy $\tilde{\omega}_{pi}$, where (Kwei *et al* 1988, Lindhard and Scharff 1953)

$$\tilde{\omega}_{pi} = (\omega_{pi}^2 + \omega_i^2)^{1/2} \tag{3}$$

and ω_i is the binding energy of the ith subshell. At $k \to \infty$, ω_{ki} tends to the Bethe ridge (Inokuti 1971), i.e. a region in the neighbourhood of the free electron dispersive line $k^2/2$. With this guidance, one may write

$$\omega_{ki} = \tilde{\omega}_{pi} + \alpha_i(k)k^2/2 \tag{4}$$

where $\alpha_i(k)$ is a weakly k-dependent function and $\alpha_i(\infty) = 1$ as is required. Substituting (2) into (1), one obtains

$$\frac{\partial f}{\partial \omega}(k, \omega) = \sum_i \frac{\partial f_i}{\partial \omega}(k, \omega) = \sum_i \frac{2Z_i}{\pi} \frac{\omega^2 \gamma_{ki}}{(\omega^2 - \omega_{ki}^2)^2 + \omega^2 \gamma_{ki}^2}. \tag{5}$$

It is found in (5) that the GOS is separated into contributions from individual subshells.

Now, consider the electron density distribution of the ith subshell, $n_i(r)$, varying with the radius from the nucleus. Applying the LPA procedure, i.e. averaging the local GOS over the entire space occupied by an atom according to the space-varying electron density distribution, one obtains the LPA GOS of the ith subshell as

$$\frac{\partial f_i}{\partial \omega}(k, \omega) = \frac{2}{\pi} \int \frac{4\pi r^2 n_i(r) \omega^2 \gamma_{ki}}{\{\omega^2 - [\tilde{\omega}_{pi}(r) + \alpha_i(k) k^2/2]^2\}^2 + \omega^2 \gamma_{ki}^2} \, dr. \tag{6}$$

Equation (6) represents an average GOS of bound local plasmas with density $n_i(r)$ and binding energy ω_i. In the limit of zero momentum transfer, this equation leads to equation (19) of Kwei *et al* (1988).

Note that the atomic GOS calculated using equation (6) satisfies the sum rule

$$\int \frac{\partial f_i}{\partial \omega}(k, \omega) \, d\omega = \int 4\pi r^2 n_i(r) \, dr = Z_i. \tag{7}$$

However, the LPA concept is valid only for GOS contributed by ionisations but not for discrete excitations. Let $Z_i^{\mathrm{I}}(k)$, $Z_i^{\mathrm{U}}(k)$ and $Z_i^{\mathrm{O}}(k)$ be the sum oscillator strength contributed by ionisations, excitations to unoccupied levels and excitations to occupied levels respectively. They are defined by (McGuire *et al* 1982, McGuire 1983)

$$Z_i^{\mathrm{I}}(k) = \int \frac{\partial f_i^{\mathrm{I}}}{\partial \omega}(k, \omega) \, d\omega \tag{8}$$

$$Z_i^{\mathrm{U}}(k) = \sum_{\text{unoccupied } i'} f_{i,i'}(k, E_i - E_{i'}) \tag{9}$$

and

$$Z_i^{\mathrm{O}}(k) = \sum_{\text{occupied } i'} f_{i,i'}(k, E_i - E_{i'}) \tag{10}$$

where $\partial f_i^{\mathrm{I}}/\partial \omega$ is the ionisation GOS and $f_{i,i'}$ is the excitation GOS for the transition between initial i and final i' states. The sum rule of (7) is equivalent to the relation $Z_i = Z_i^{\mathrm{I}}(k) + Z_i^{\mathrm{U}}(k) + Z_i^{\mathrm{O}}(k)$. The correct ionisation GOS is therefore established by multiplying (6) by an ionisation fraction defined by $F_{\mathrm{I}}(k) = Z_i^{\mathrm{I}}(k)/Z_i$. Thus, we obtain

$$\frac{\partial f_i^{\mathrm{I}}}{\partial \omega}(k, \omega) = \frac{2}{\pi} \int \frac{4\pi r^2 n_i^{\mathrm{I}}(r, k) \omega^2 \gamma_{ki}}{\{\omega^2 - [\tilde{\omega}_{pi}(r) + \alpha_i(k) k^2/2]^2\}^2 + \omega^2 \gamma_{ki}^2} \, dr \tag{11}$$

where $n_i^{\mathrm{I}}(r, k) = n_i(r) F_{\mathrm{I}}(k)$.

Taking $k = 0$ and $\gamma_{ki} \to 0$, (11) leads to

$$\frac{\partial f_i^{\mathrm{I}}}{\partial \omega}(0, \omega) = \frac{4\pi r_0^2 n_i^{\mathrm{I}}(r_0, 0)}{|\tilde{\omega}_{pi}'(r_0)|} \tag{12}$$

where $\tilde{\omega}_{pi}'(r_0)$ is the derivative of $\tilde{\omega}_{pi}(r)$ at r_0 and r_0 is the root of the equation

$$\omega - \tilde{\omega}_{pi}(r) = 0. \tag{13}$$

One may obtain a so-called pseudo-electron density distribution $n_i^1(r, 0)$ (Penn 1987) from equations (12), (13) and (3) by substituting experimental or theoretical ionisation GOS data into the left-hand side of (12). The pseudo-electron density represents a hypothetical electron density which yields the experimental or theoretical GOS at zero momentum transfer under the LPA approach.

The plasma damping coefficient in (11) controls the width of the GOS spectrum. It has been shown (Ashley and Williams 1980) that this coefficient was directly related to the full width at half maximum of the GOS spectrum. From an examination of McGuire's GOS data (McGuire 1971), it reveals that this coefficient is increasing with the momentum transfer. In a first approximation, one may propose $\gamma_{ki} = A_i + B_i k^2$ (Zacharias 1972), where A_i and B_i are coefficients depending on the atom and the subshell. Since the pseudo-electron density distribution is derived under the condition $\gamma_{ki} \to 0$ at $k = 0$, $A_i = 0$ follows accordingly, and in this work we use

$$\gamma_{ki} = B_i k^2. \tag{14}$$

3. Results and discussion

Figure 1 shows a plot of GOS for the carbon 1s shell calculated by McGuire (1971) using the matrix element method and the Hartree-Slater potential wavefunctions (Herman and Skillman 1963). It is seen that the GOS spectra for small momentum transfers decrease monotonically with the increase of energy transfer. As the momentum transfer becomes larger and larger, these spectra become bell shaped with the width increasingly broader, the height smaller and the peak energy transfer greater. This indicates that the plasma damping coefficient approaches zero at the smallest available

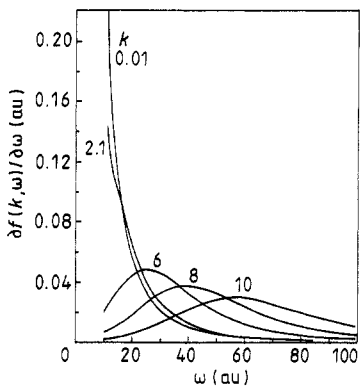

Figure 1. A plot of ionisation GOS for the carbon K shell from the matrix element method (McGuire 1971). All quantities are in atomic units.

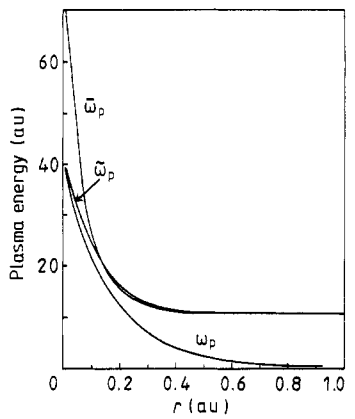

Figure 2. A comparison of the local plasma energy, $\omega_p(r)$, the effective plasma energy, $\tilde{\omega}_p(r)$, and the pseudo-effective plasma energy, $\bar{\omega}_p(r)$ for the carbon K shell. $\omega_p(r) = (4\pi n(r))^{1/2}$ and $\tilde{\omega}_p(r) = (4\pi n(r) + \omega_{C-1s}^2)^{1/2}$ are calculated using the Hartree-Slater electron density distribution (Herman and Skillman 1963). $\bar{\omega}_p(r) = (4\pi n^1(r, 0) + \omega_{C-1s}^2)^{1/2}$ is calculated using (12) with ionisation GOS at $k = 0.01$ from the matrix element method (McGuire 1971). All quantities are in atomic units.

k value of 0.01. Therefore, we may substitute the GOS values at $k = 0.01$ into equation (12) to determine the pseudo-electron density and subsequently the pseudo-effective plasma energy using (3). Figure 2 is a comparison of the results on the free electron plasma energy $\omega_p(r)$, the bound electron effective plasma energy $\tilde{\omega}_p(r)$ and the pseudo-effective plasma energy $\bar{\omega}_p(r)$, where $\omega_p(r)$ and $\tilde{\omega}_p(r)$ are calculated using the HFS electron densities and $\bar{\omega}_p(r)$ using McGuire's GOS data at $k = 0.01$. At small radius the free electron plasma energy dominates the contribution to the effective plasma energy according to (3), whereas the binding energy dominates at large radius. Substantial differences between $\tilde{\omega}_p(r)$ and $\bar{\omega}_p(r)$ occur only at small r where at $r \to 0$ $\tilde{\omega}_p$ extends to a finite value and $\bar{\omega}_p$ extends to infinity. Since the GOS is inversely proportional to the first derivative of $\tilde{\omega}_p$ as expressed in (12), large values of $\tilde{\omega}_p'$ at small r correspond to small GOS at large ω in figure 1. On the other hand, small values of $\tilde{\omega}_p'$ at large r correspond to large GOS at small ω in figure 1.

It is seen from figure 1 that plasma damping becomes more and more important as k becomes larger and larger. Areas under the GOS spectra for different k values are constrained by the sum rule of (8). To study the dependence of the plasma damping coefficient on the momentum transfer, we replot the data presented in figure 1 as a function of a scaled energy transfer defined by $\omega/(\omega_{C-1s}+k^2/2)$, where ω_{C-1s} is the binding energy of the carbon 1s-shell. This is shown in figure 3 where the ordinate is taken as the product of GOS and $\omega_{C-1s}+k^2/2$ in order to retain areas under the spectra unchanged from those in figure 1. One advantage of the plot associated with figure 3 is that all spectra have maxima at about the same scaled energy transfer around 1. Except for spectra at $k = 0.01$ and 2.1, all other spectra have nearly equal widths. This confirms the assumption of (14).

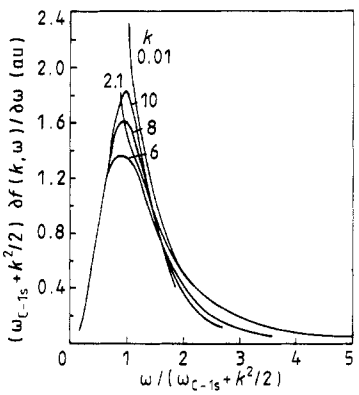

Figure 3. A new plot of the data presented in figure 1. The energy transfer on the abscissa is scaled by dividing ω by $\omega_{C-1s}+k^2/2$. The ordinate is taken as the product of GOS and $\omega_{C-1s}+k^2/2$. All quantities are in atomic units.

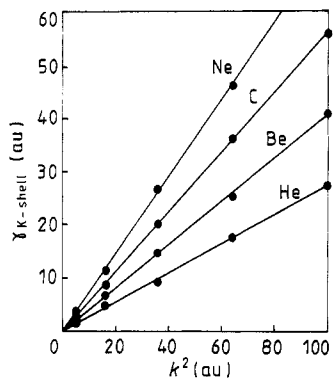

Figure 4. A plot of the plasma damping coefficient as a function of momentum transfer squared for the K shell of several atoms. Results (full circles) are obtained by a fit of equation (11) to ionisation GOS from the matrix element method (McGuire 1971). All quantities are in atomic units.

To this end we have calculated ionisation GOS of the K shell using (11) with parameters determined by a fit of this equation to McGuire's GOS data. Figure 4 shows a representation of the fitted results (full circles) for the plasma damping coefficient as a function of momentum transfer squared. Note that we have assumed in (11) $n_i^I(r, k) = \beta_i(k) n_i^I(r, 0)$, where $\beta_i(k)$ is determined from the fitting procedure and $n_i^I(r, 0)$

is calculated using (12) and the $k = 0.01$ GOS of McGuire. Since this assumption is based on the pseudo-electron density distribution corresponding to zero plasma damping coefficient at zero momentum transfer, A_i in (14) thus vanishes. This leads to straight lines passing through the origin in the plot of figure 4. It indicates in the figure that slopes of these lines increase with atomic number of the atom. To see the dependence of this increase, we plot in figure 5 these slopes, or B_i in (14), as a function of binding energy of the K-shell. It reveals that a log-log dependence of B_i on the binding energy is effective. Such a dependence leads to an easy determination of the plasma damping coefficient at any momentum transfer for any atom.

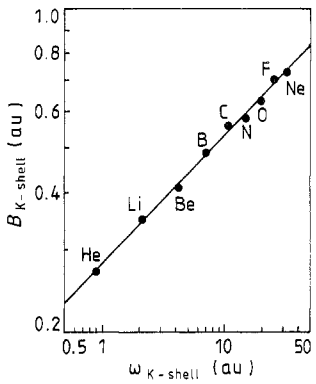

Figure 5. A plot of slopes of the straight lines presented in figure 4 plotted against the binding energy of the K shell of atoms. All quantities are in atomic units.

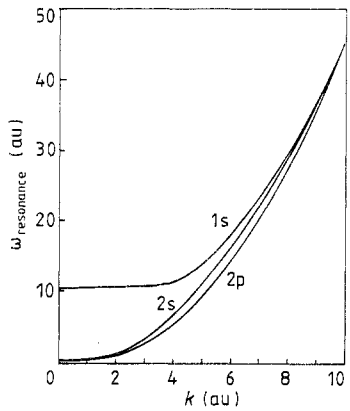

Figure 6. A plot of the resonant energy transfer, $\omega_i + \alpha_i(k)k^2/2$, as a function of momentum transfer squared for all subshells of the carbon atom. All quantities are in atomic units.

The value of $\alpha_i(k)$ in (11) has also been determined by a fit of this equation to McGuire's GOS data. As discussed previously, α_i increases with k and eventually approaches 1 at $k \to \infty$. A plot of the fitted results on the resonant energy transfer at $r \to \infty$, i.e. $\omega_i + \alpha_i(k)k^2/2$ according to (3) and (11), for the carbon atom is shown in figure 6. It is seen that this energy, representing the energy transfer corresponding to the maximum GOS at a given k, approaches the binding energy at $k = 0$ and tends to merge with the Bethe ridge at $k \to \infty$. The resonant energy transfer at smaller r, $\tilde{\omega}_{pi}(r) + \alpha_i(k)k^2/2$, is larger because of the increased contribution of plasma oscillations as shown in figure 2.

With all parameters determined, we have calculated using (11) ionisation GOS at any momentum transfers and energy transfers for the K shell. Representative results as a function of energy transfer for several momentum transfers for the carbon and beryllium atoms are plotted in figures 7 and 8 and compared with corresponding results of the matrix element method. Fairly reasonable agreement is found for all cases. In figure 9, we plot a representation of the calculated ionisation GOS for the neon K shell against momentum and energy transfers. One sees that when k is small, the GOS has a prominent maximum at an energy transfer around the binding energy. This maximum corresponds to the threshold energy transfer involved in the quantum ionisation of atoms. The extended tail of the GOS spectrum corresponds to the contribution from damped local plasmas. As k increases, this spectrum becomes further broadened with the dispersive line in (k, ω) plane featuring a free electron behaviour.

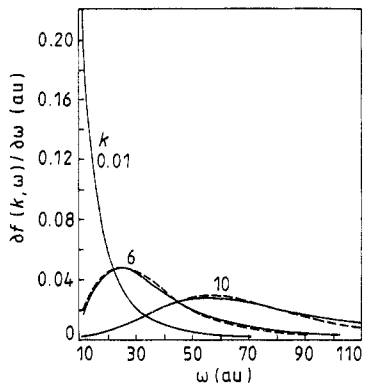

Figure 7. A comparison of ionisation GOS of the carbon K shell calculated in this work (full curves) and those from the matrix element method (McGuire 1971) (broken curves). All quantities are in atomic units.

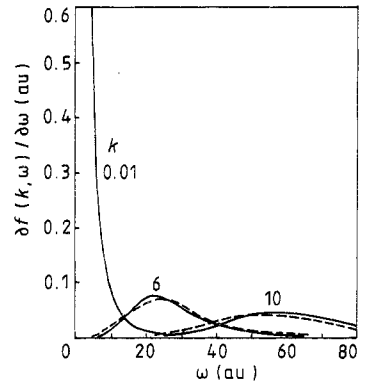

Figure 8. A comparison of ionisation GOS of the beryllium K shell calculated in this work (full curves) and those from the matrix element method (McGuire 1971) (broken curves). All quantities are in atomic units.

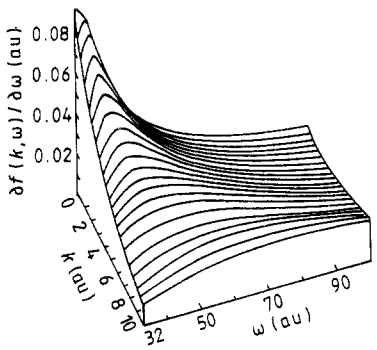

Figure 9. A representation of calculated ionisation GOS against momentum and energy transfers for the neon K shell. All quantities are in atomic units.

4. Problems with the L shell

For the L shell of atoms, the pseudo-electron density distribution derived based on the zero plasma damping coefficient is no longer valid. This can be understood from a plot of ionisation GOS for the oxygen 2s subshell of the matrix element method, shown in figure 10. The GOS spectrum corresponding to the smallest available k value of 0.01 indicates a large plasma damping coefficient with respect to the scaled energy transfer. It also indicates that (14) is poor in describing the momentum-dependent plasma damping coefficient and that a factor proportional to the fourth power of the momentum transfer may be essential. Although the pseudo-electron density distribution does not necessarily reflect the actual electron density distribution, the difference between them may indicate the applicability of the former distribution in the LPA. In figure 11, we plot a comparison of these distributions for the nitrogen atom. The profound differences for the 2s and 2p subshells are due to the non-zero plasma damping coefficient at $k \rightarrow 0$ and the correlation of electrons in these subshells (Kwei *et al* 1988). Because of these, a different approach should be sought in the application of LPA for the L shell. We will discuss this approach in detail in a later paper.

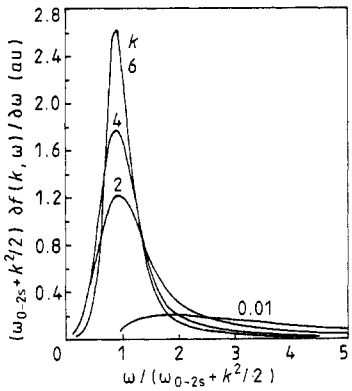

Figure 10. A similar plot to figure 3 for ionisation GOS of the oxygen 2s subshell from the matrix element method (McGuire 1971). All quantities are in atomic units.

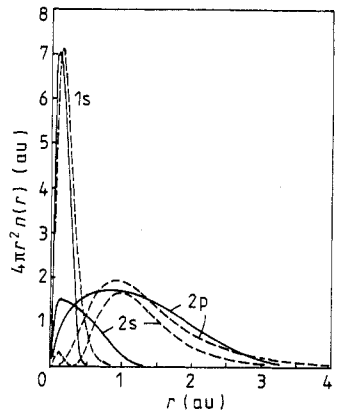

Figure 11. A comparison of the pseudo-electron density distribution (full curves) and the Hartree-Slater electron density distribution (broken curves) (Herman and Skillman 1963) for the nitrogen atom. All quantities are in atomic units.

5. Conclusion

The LPA has proved in this work to be applicable in evaluating ionisation GOS at any momentum transfers and energy transfers for the atomic K shell. The pseudo electron density distribution was demonstrated to be useful in the procedure of the LPA for averaging momentum-dependent GOS. The plasma damping coefficient was found proportional to the momentum transfer squared with the proportional constant relating directly to the binding energy of the atom.

Because of the problems discussed in section 4, a different approach should be sought in the application of LPA for the L shell. We will discuss this approach in a later paper.

References

Ashley J C and Williams M W 1980 *Radiat. Res.* **81** 364
Bethe H 1930 *Ann. Phys., Lpz.* **5** 325
—— 1933 *Handbuch der Physik* vol 24 (Berlin: Springer)
Dehmer J L, Inokuti M and Saxon R P 1975 *Phys. Rev.* A **12** 102
Gryzinski M 1965a *Phys. Rev.* **138** A305
—— 1965b *Phys. Rev.* **138** A322
—— 1965c *Phys. Rev.* **138** A336
Herman F and Skillman S 1963 *Atomic Structure Calculations* (New York: Prentice-Hall)
Inokuti M 1971 *Rev. Mod. Phys.* **43** 297
Inokuti M, Baer T and Dehmer J L 1978 *Phys. Rev.* A **17** 1229
Johnson R E and Inokuti M 1983 *Comment. At. Mol. Phys.* **14** 19
Kwei C M, Lin T L and Tung C J 1988 *J. Phys. B: At. Mol. Opt. Phys.* **21** 2901
Lindhard J and Scharff M 1953 *K. Danske Vidensk. Selsk. Mat.-Fys. Medd.* **27** 1
McGuire E J 1971 *Phys. Rev.* A **3** 267
—— 1983 *Phys. Rev.* A **28** 49
McGuire E J, Peek J M and Pitchford L C 1982 *Phys. Rev.* A **26** 1318
Penn D R 1987 *Phys. Rev.* B **35** 482
Powell C J 1985 *Electron Impact Ionization* (New York: Springer) p 198

Raether H 1980 *Excitation of Plasmons and Interband Transitions by Electrons* (Springer Tracts in Modern Physics vol 88) (Berlin: Springer)
Ritchie R H and Howie A 1977 *Phil. Mag.* **36** 463
Tung C J 1980 *Phys. Rev.* A **22** 2550
Tung C J and Kwei C M 1985 *Nucl. Instrum. Methods* B **12** 464
Tung C J, Shyu R L and Kwei C M 1988 *J. Phys. D: Appl. Phys.* **21** 1125
Walske M C 1952 *Phys. Rev.* **88** 1283
—— 1956 *Phys. Rev.* **101** 940
Zacharias P 1972 *Z. Phys.* **256** 92